3-1-2016

Pulmonary CT and MRI phenotypes that help explain chronic pulmonary obstruction disease pathophysiology and outcomes

Eric A Hoffman

David A Lynch

R Graham Barr

Edwin J R van Beek

Grace Parraga

Pulmonary CT and MRI Phenotypes That Help Explain Chronic Pulmonary Obstruction Disease Pathophysiology and Outcomes

Eric A. Hoffman, PhD,[1,2,3] David A. Lynch, MD,[4] R. Graham Barr, MD,[5,6] Edwin J.R. van Beek, MD,[7] Grace Parraga, PhD,[8,9]* for the IWPFI Investigators

Pulmonary x-ray computed tomographic (CT) and magnetic resonance imaging (MRI) research and development has been motivated, in part, by the quest to subphenotype common chronic lung diseases such as chronic obstructive pulmonary disease (COPD). For thoracic CT and MRI, the main COPD research tools, disease biomarkers are being validated that go beyond anatomy and structure to include pulmonary functional measurements such as regional ventilation, perfusion, and inflammation. In addition, there has also been a drive to improve spatial and contrast resolution while at the same time reducing or eliminating radiation exposure. Therefore, this review focuses on our evolving understanding of patient-relevant and clinically important COPD endpoints and how current and emerging MRI and CT tools and measurements may be exploited for their identification, quantification, and utilization. Since reviews of the imaging physics of pulmonary CT and MRI and reviews of other COPD imaging methods were previously published and well-summarized, we focus on the current clinical challenges in COPD and the potential of newly emerging MR and CT imaging measurements to address them. Here we summarize MRI and CT imaging methods and their clinical translation for generating reproducible and sensitive measurements of COPD related to pulmonary ventilation and perfusion as well as parenchyma morphology. The key clinical problems in COPD provide an important framework in which pulmonary imaging needs to rapidly move in order to address the staggering burden, costs, as well as the mortality and morbidity associated with COPD.

J. MAGN. RESON. IMAGING 2016;43:544–557.

Copd Measurements and Endpoints are Urgently Needed

Despite decades of research, therapies that modify chronic obstructive pulmonary disease (COPD) progression or mortality are lacking.[1] Despite considerable efforts to discover and develop new COPD interventions, progress has been slow. This is in large part due to limited and suboptimal patient phenotyping that relies on spirometry measurements made at the mouth that cannot account for the regional and intersubject variability of COPD. Moreover, while COPD is still diagnosed and classified on the basis of symptoms related to the presence of persistent airflow limitation,[1] these measurements correlate weakly with important clinical outcomes.[2]

A wide variety of imaging methods may be used to study the pulmonary system, including those that rely on tissue absorption of x-ray radiation (chest x-ray and computed tomography [CT]), radiofrequency stimulation (magnetic resonance imaging [MRI]), or signals generated from injected or inhaled radioactive particles (simple gamma emission projection imaging, single photon emission tomography [SPECT] and positron emission tomography [PET]) and inhaled or

View this article online at wileyonlinelibrary.com. DOI: 10.1002/jmri.25010

Received Apr 22, 2015, Accepted for publication Jul 1, 2015.

*Address reprint requests to: G.P., Robarts Research Institute, 1151 Richmond St. N, London, Canada N6A 5B7. E-mail: gparraga@robarts.ca

From the [1]Department of Radiology, University of Iowa, Iowa City, Iowa, USA; [2]Department of Internal Medicine, University of Iowa, Iowa City, Iowa, USA; [3]Department of Biomedical Engineering, University of Iowa, Iowa City, Iowa, USA; [4]Department of Radiology, National Jewish Health Center, Denver, Colorado, USA; [5]Division of General Medicine, Division of Pulmonary, Allergy and Critical Care, Department of Medicine, Columbia University Medical Center, New York, New York, USA; [6]Department of Epidemiology, Columbia University Medical Center, New York, New York, USA; [7]Clinical Research Imaging Centre, Queen's Medical Research Institute, University of Edinburgh, Scotland, UK; [8]Robarts Research Institute, University of Western Ontario, London, Canada; and [9]Department of Medical Biophysics, University of Western Ontario, London, Canada

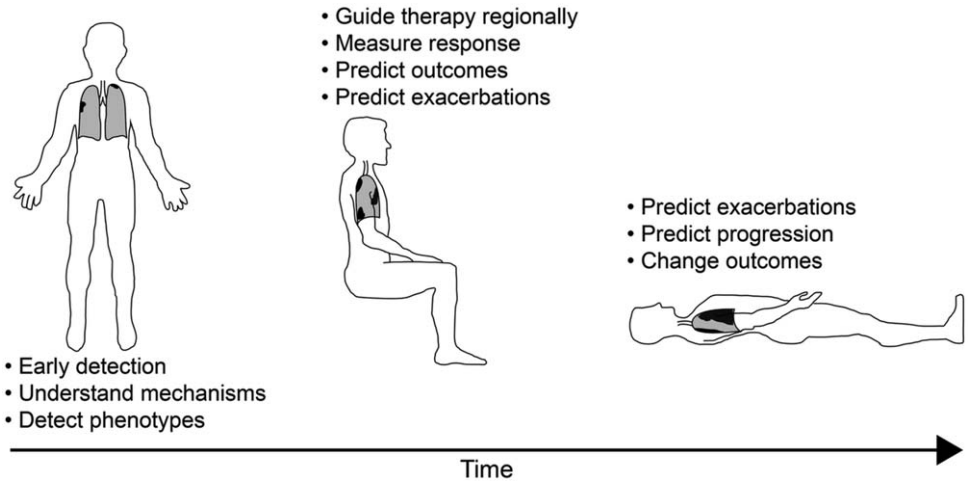

FIGURE 1: Current COPD challenges. Three distinct COPD phases are outlined in schematic: 1) Early disease when patients are asymptomatic, clinical measurements typically do not reflect disease but imaging measurements provide evidence of mild emphysema, airways disease, perfusion heterogeneity, LV filling defects, etc. 2) Mild-moderate COPD as patients become symptomatic, clinical measurements are modestly abnormal while imaging measurements can be markedly abnormal revealing regional disease, LV filling defects can continue to worsen, comorbidities can begin to appear including aortic aneurysms, coronary disease, lung nodules, and osteoporosis. 3) Severe COPD with patients reporting severe symptoms and activity impairment, clinical measurements of airflow limitation, diffusing capacity of carbon monoxide, and gas trapping are markedly abnormal and yet patients still can be differentiated into those with predominantly airway or predominantly parenchymal disease with marked differences in the distribution of parenchymal destruction.

injected contrast agents. New insights into the basis for disease initiation and progression using these methods have the potential to break through the current conundrum, which is the fact that image acquisition and analysis tools are slow to be adopted because of a lack of meaningful interventions and yet the interventions are slow in coming because of a lack of understanding disease mechanisms and etiology. Therefore, as shown in Fig. 1, we frame this review of CT and MRI measurements and phenotypes as potential solutions to the following major COPD problems: 1) COPD treatments are required that improve outcomes, not just symptoms; 2) a better understanding of COPD disease onset and mechanisms is urgently required in order to better design drugs targeted at underlying pathophysiology; 3) more sensitive measurements are required to better understand the links between ventilation, perfusion, and inflammation; and 4) better predictive measurements of COPD exacerbations and progression are critically needed. Here we summarize and compare MRI and CT tools and measurements of COPD because of their near-universal availability that makes their use in COPD multicenter clinical trials and COPD patient care both practical and timely. Taken together, MRI and CT methods provide a way to identify the underlying pathologies associated with COPD and previous work has been summarized and previously reviewed.[3–5]

Pulmonary CT Measurements of Copd

CT Structural Measurements and Phenotypes

Computer-based methods[6–9] for the objective quantitation of CT images are increasingly used in multicenter studies[10–15] that aim to interrogate phenotype–genotype linkages and identify intermediary endpoints for the assessment of potential interventions. A cornerstone of this approach is the CT lung tissue attenuation or density mask that provides a way to estimate regional COPD-related emphysema. By empirically defining regional emphysematous lung using selected threshold tissue attenuation measurements (Hounsfield Unit [HU]) at full inspiration (total lung capacity [TLC]), one can count the number of voxels in the whole lung and express this measure. In this way, the percent of voxels reflecting emphysema can be expressed relative to the total volume of the lung or lung region.[16–23] The CT density mask is particularly useful in classifying mild/moderate and severe emphysema[24,25] and has been used in the National Emphysema Treatment Trial (NETT) to identify subgroups of patients who show benefit from lung volume reduction surgery.[26] In the left panel of Fig. 2 (using Apollo software provided by VIDA Diagnostics, Coralville, IA), the spatially heterogeneous distribution of emphysema, shown in spheres and regional clustering (sphere size), is shown by lung lobe. Similarly, a density mask may be used on the expiratory dataset (residual volume [RV] or functional residual capacity [FRC]) to identify regions of air trapping as shown in the middle panel of Fig. 2. In both the inspiratory and expiratory images, airways may also be segmented and labeled[9,27,28] using commercially available software such that relationships can be determined between the airway path, airway remodeling features, and parenchymal destruction or peripheral airway closure. CT-based density metrics have been used in numerous large-scale studies,[12–15] producing a wealth of literature over the past several years. These measures have identified correspondence of quantitative CT measures of emphysema and air trapping to, for example: genotypes,[29,30]

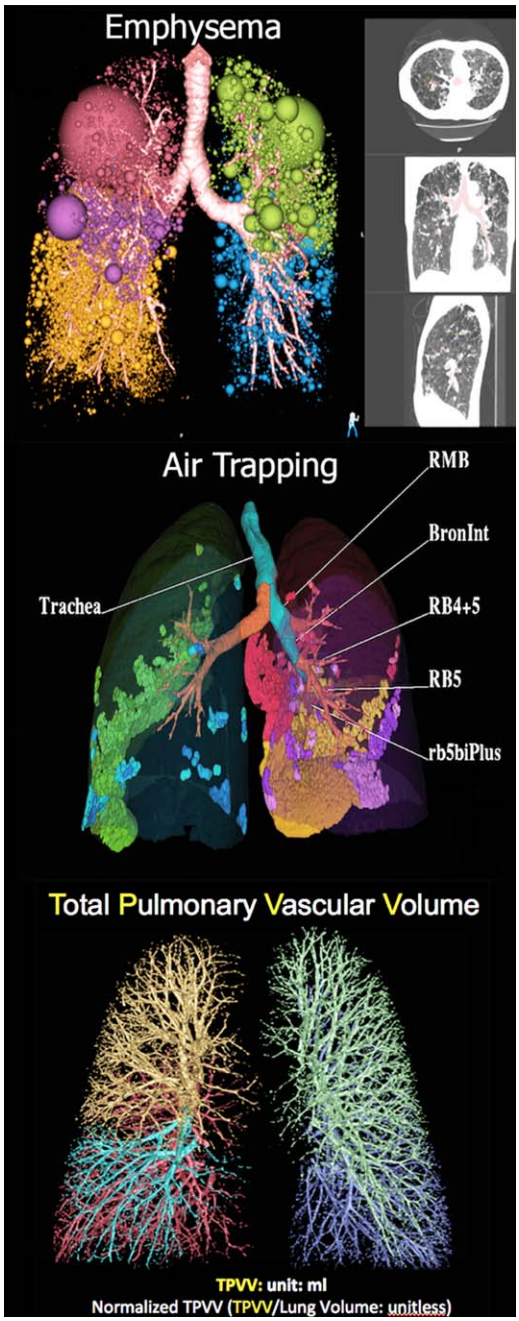

FIGURE 2: CT measurements: Threshold-based evaluation of the extent and distribution of emphysema at full inspiration (top panel), amount and air trapping at expiration to functional residual capacity (FRC) or residual volume (RV) (middle panels), airway geometry assessed in conjunction with distribution patterns of emphysema and air trapping (middle panels), vascular anatomy (total pulmonary vascular volume and total pulmonary arterial volume assessed from full inspiratory noncontrast-enhanced CT scans (bottom panel). Color-coding differentiates between lung lobes.

left ventricular (LV) filling,[31] physiologic measures,[32,33] environmental smoke exposure in childhood as a risk factor for emphysema,[34] predictors of bronchoreversibility,[35] association of cigarette smoking with subclinical disease,[36] and trapped gas in severe asthma.[37] It is also important to note that in addition to tissue attenuation or density masks, texture analyses may be employed to evaluate clusters of emphysema[38] such as estimated using low attenuating clusters. Image analysis methods based on such local feature patterns provide a way to objectively differentiate between these subtypes and some of these methods have better classification rates than expert radiologists.[39] So-called low attenuation clusters are visually obvious, correlating with histopathology measurements[40] and more closely reflecting scoring performed by a radiologist.[41]

However, CT quantification of the lung parenchyma is also challenging. Scanner miscalibration, inconsistent use of reconstruction kernels, differences in reconstruction algorithms between manufacturers, and poor coaching of the patient to the targeted lung volume can result in measurement variability.[42–45] Accurate, quantitative CT requires image acquisition consistency,[46] and even then, subject age, sex, race/ethnicity, and height influence the normal range of these measures (similar to lung function) as does weight.[47] Current smoking status has a large and paradoxical effect on these measures,[47] making precise measurements of smoking status (eg, cotinine or other objective measure) important in longitudinal studies. Reference equations for both percent emphysema and total lung volume on CT are now available to account for most of these differences.[47] The limitations due to concerns of radiation dose are being addressed with recent advances in CT technologies, including improvements in the x-ray tube, detector technology, adaptive exposure,[48,49] and iterative image reconstruction,[50–54] leading to clinically adequate image quality with sub-mSv doses.[48,55] Finally, despite considerable successes using quantitative CT to assess the presence and distribution of emphysema and airway wall remodeling,[56–61] critical underlying differences among disease subpopulations continue to emerge. For example, in an apparently discordant result, spatially matched airway segmentation demonstrated that airway walls may become thinner rather than thicker in COPD, leaving open the possibility that airway wall remodeling may itself have multiple phenotypes.[9]

Functional CT Measurements and Phenotypes

PULMONARY CT VASCULAR OR PERFUSION. It has long been thought that a better understanding of the pathologic response to inflammation in COPD and asthma will be important for the design of new therapies. What is well understood is that in response to noxious particles and gases in cigarette smoke, the lung reacts by recruiting inflammatory cells. Pulmonary vascular changes, including thickening of the vessel walls, have been characterized early in the history of COPD.[62,63] More recently it was observed that in the presence of inflammation there is an enhanced delivery of progenitor cells to the lung.[64,65] Remy-Jardin et al[66] recently observed an increased propensity for the lung to develop emphysema in regions of suspected inflammatory processes as

defined by ill-defined ground-glass opacities and micronodules. In more than half of smokers, the inflammatory process was able to resolve itself with repair and maintenance of normal parenchymal anatomy and function. For the remainder (30–45% of smokers) there was parenchymal destruction. There is evidence in the literature suggesting that in humans and animals, hypoxic pulmonary vasoconstriction (HPV) is normally blocked in the presence of inflammation.[25,67–69] For example, Alford et al[70] demonstrated that smokers with normal pulmonary function, but small visibly obvious signs of localized, apical centrilobular emphysema, have an increase in coefficient of variation (CV) of CT-based regional pulmonary blood flow (PBF) and mean transit time (MTT), supporting a hypothesis that one etiology of smoking-associated emphysema may be failure to maintain PBF to inflamed lung regions. Recent work published together with an associated editorial[31,71] also demonstrated and discussed the strong relationship between impaired LV filling and percent emphysema in a group of nonsmokers, exsmokers, and current smokers. The correlation between impaired LV filling with emphysema was greatest in current smokers compared with previous smokers, consistent with the notion that the inflammatory effects of smoking may determine this effect rather than emphysema alone.

With the observation that pulmonary perfusion heterogeneity may serve as a biomarker in smokers susceptible to centrilobular emphysema,[70] it has been hypothesized that the lung normally inhibits HPV in the presence of inflammation. Conversely, in patients unable to block HPV in inflamed lung regions, perfusion is reduced, thus prolonging inflammation and limiting repair mechanisms. With the use of single-breath methods in conjunction with dual energy CT, efforts have been directed towards maintaining sensitivity to increased perfusion heterogeneity while simplifying imaging methodologies.

Dual-energy CT (DECT) provides a way to double the temporal resolution of CT, making it possible to image the entire lung field with a 0.62-mm slice thickness in 0.6 seconds. By having two x-ray guns together with two sets of detector rows, both capable of acquiring 128 slices of image data, there is now the possibility of DECT which allows for sensitive discrimination between tissue types and contrast agents such as iodine for perfusion and xenon (Xe) for ventilation. At two different peak kilo-voltages (kVp), the reconstructed CT densities for iodine or Xe are shifted significantly between the two resultant image datasets, but the body tissues are not. Thus, because the two image sets were acquired simultaneously, assuring alignment, with a modified form of image subtraction (material decomposition), it is possible to assess perfused blood volume or regional ventilation, respectively. For regional assessment of perfused blood volume, when blood is equilibrated with a concentration of iodine (or gadolinium) through the slow infusion of contrast agent, an image of iodine (or gadolinium) can be directly related to regional blood volume.

Other studies have demonstrated the equivalency of perfused blood volume (PBV), as assessed by DECT, and true perfusion. PBV and PBF likely reflect one another because peripheral vascular beds dilate and capillary beds are recruited with increased PBF. PBV may be evaluated using DECT during a slow infusion of x-ray contrast. As shown in Fig. 3, modified[72] from a report on interventions performed in pigs, regional perfusion (color-coded from red to blue as percent of total perfused blood volume or total perfusion) was perturbed either by incrementally pulling back a balloon catheter placed in a pulmonary artery or by imaging the lung at various static inflation pressures which effectively reduces perfusion in the nondependent lung regions.[72] Under all conditions, PBF maps and PBV maps are strikingly similar and a strong relationship for PBF and PBV heterogeneity was also demonstrated.

PULMONARY CT VENTILATION. Xe gas regional wash-in and washout kinetic studies were also explored using CT imaging[73–75] and these methods have been translated clinical studies.[76–82] Importantly, with the more recent development of DECT, it is possible to simplify the assessment of regional ventilation via use of single-breath methods. As shown in Fig. 4, by adjusting Xe inhalation of a Xe/O_2 gas mixture, gas flow to the central airways may be monitored and compared with gas flow to the parenchyma. As shown in Fig. 4, left panel, the central airway tree is identified by having the subject inhale to TLC, exhale the central dead space volume, and reinhale the same volume of a Xe gas mixture. This leaves just the central airways filled with Xe gas. In the right panel, results are shown from a single inhalation of a Xe gas mixture. It was also demonstrated that with a slow inhalation of Xe gas mixtures, geometry, and gas density influence or dominate gas distribution causing increased ventilation heterogeneity, while with a rapid inspiration, ventilation is more homogeneous.[83] Furthermore, the gravity-driven distribution of Xe gas can be eliminated by mixing Xe with helium (He), likely due to the change in the gas density mixture. Another contrast gas agent, krypton (Kr), while less radiodense than Xe,[84,85] has no anesthetic effects. As multispectral CT technologies, including photon counting CT,[86–88] evolve, it is expected that sensitivity to Kr gas contrast will improve, making it a potential translational/clinical method.

As an alternative to inhaled contrast agents, recent studies[89,90] have shown that regional measures of lung ventilation can be assessed using CT images acquired at different volumes without the need for inhaled contrast agents. A two-lung volume (TLC or full inspiration and RV or full expiration) protocol has been standardized as part of "SPIROMICS",[13] a CT protocol that obtains isotropic submillimeter images of the

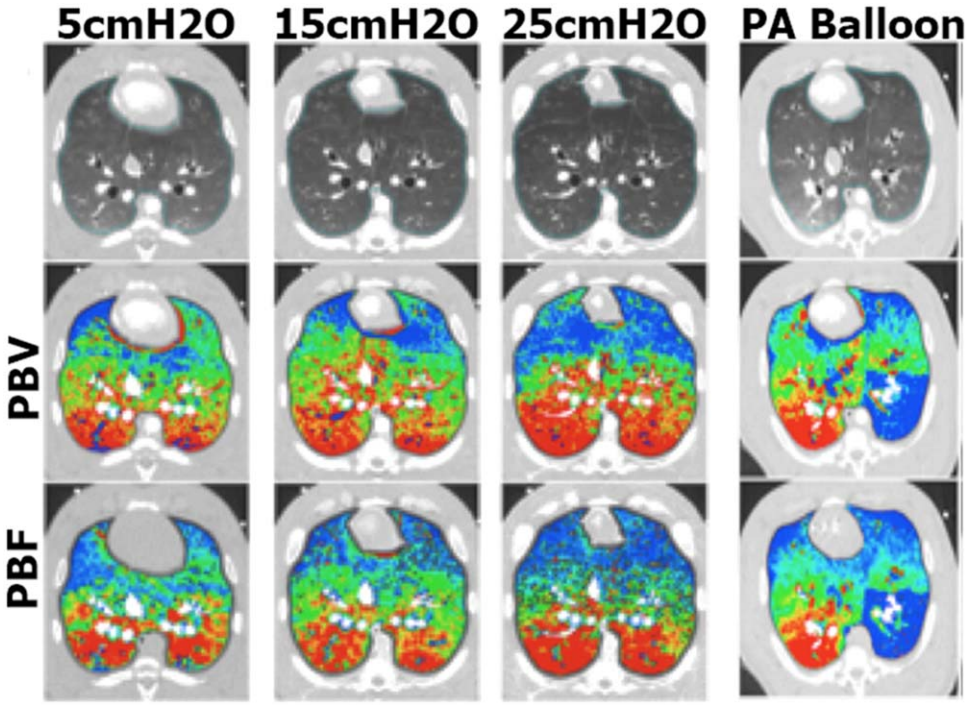

FIGURE 3: Gray-scale (top row), PBV (middle row), and PBF (lower row) MDCT scans (Columns 1–3). Color map comparison of CT-derived PBF and PBV from pig imaged at three different lung volumes, used to achieve a range of pulmonary perfusion values (Column 4). Color map comparison of CT-derived PBF (dynamic axial scanning) and PBV (dual energy spiral scanning) from pig studied with a balloon partially inflated in a left lower lobe pulmonary artery. Color coding is the same for each condition: percent of total PBV or PBV with low values in blue and high values in red. Modified from Ref. [72].

entire lungs at TLC and RV. Using this protocol together with advanced image registration methods,[90–95] regional maps of lung ventilation can be obtained at spatial resolutions close to the size of a pulmonary acinus. Image matching of an inspiratory/expiratory lung image pair has also been employed[7] to help differentiate air trapping from emphysema. Functional measurements may be directly generated from expiratory CT[96,97] or a combination of inspiratory and expiratory CT, including those generated using parametric response maps.[7] All of these important approaches have the potential to test

FIGURE 4: DECT scans of the airway tree (left) and lung parenchyma (right) of an anesthetized pig. For the scan in the left panel, the lung was inflated to 25 cmH_2O airway pressure using room air. An amount of air approximately equal in volume to the central airway tree was removed and replaced with xenon gas. This provided a way to identify the central airway tree without the use of more conventional airway segmentation methods. In the right panel, the lungs were inflated from functional residual capacity to total lung capacity via a gas mixture of 80% xenon and 20% oxygen. Material decomposition image processing was used to generate an image representing the regional distribution of the inhaled xenon gas.

the hypotheses generated using micro-CT[98] about the pathological mechanisms that accompany the earliest airway and parenchyma changes in COPD.

There is well-developed software commercially available for evaluating the relationship of airway microstructural abnormalities with ventilation and emerging software tools are now being developed to probe the geometry of the pulmonary arterial and venous trees and vascular–structure function relationships.[99–101] The extracted pulmonary vascular tree from a noncontrast inspiratory MDCT volume of the lung is shown in the right panel of Fig. 2, and the volume of this combined arterial and venous tree, the total pulmonary vascular volume (TPVV), has been developed using methods that segment the arterial tree[101]. The cross-sectional area of the pulmonary trunk relative to the aorta has been shown[102] to correlate with acute exacerbations in COPD patients and TPVV (normalized to total lung volume) is currently being used as an upstream marker of downstream endothelial dysfunction[103].

Pulmonary MRI Measurements of COPD

Conventional ^{1}H MRI Structural and Functional Phenotypes

As pulmonary CT continues to advance with new capabilities and lower radiation doses, pulmonary MRI has also advanced to provide complementary tools for the quantitative evaluation of lung structure and function. However, pulmonary MRI using conventional hardware platforms (^{1}H methods) is very technically challenging and therefore, currently its clinical use has been limited. These technical demands stem from the inherently low pulmonary ^{1}H abundance and corresponding low ^{1}H signal that can be measured using conventional MRI approaches. Furthermore, the multitude of lung air–tissue interfaces generate significant magnetic field distortions or susceptibility artifacts, further diminishing pulmonary ^{1}H MRI signal. For these reasons, and until recently, the major applications of conventional pulmonary ^{1}H MRI included intravenous contrast agents to evaluate pulmonary blood flow and vessel hemodynamics.[104] Methods have also been devised that combine relaxation signals and intravenous contrast that provide a way to differentiate inflammation[105], smooth muscle remodeling, edema, and mucus deposition.[104,105] Taken together, these methods provide a way to identify the underlying pathologies associated with COPD. However, because signal intensity is generally very low using ^{1}H MRI, careful calibration with other organs in the same field of view is required. In addition, because gravity-dependent changes occur, signal averaging over time may not provide physiologically relevant information in the dependent lung regions, where atelectasis may occur in minutes while supine.

Another way to address these challenges is to reduce the time (echo time [TE]) required to acquire the pulmonary MR signal. As shown in Fig. 5, conventional, ultrashort TE (UTE) pulse sequences, as suggested two decades ago[106], significantly improve pulmonary MR signal so that emphysematous regions can be identified and quantified, based on the difference between tissue-poor emphysematous bullae and more normal parenchyma. So-called ultrashort-echo or zero echo time MRI methods help address the inherent challenges of low tissue and ^{1}H density[107] by minimizing the effects of rapid MR signal decay. The relationship between MRI signal intensity and tissue density[108], as previously shown for pulmonary CT, is clearly important for further development of the method. The first studies employing UTE methods reported that the tissue density was related to MR signal[109] and T_2*. UTE MRI was also used to measure signal intensity and T_2* in emphysema[110] and showed good correlations with histological measurements, while T_2* correlated with pulmonary function measurements[111] and pulmonary signal intensity was related to tissue density, pulmonary function, and CT density measurements.[108] Very recently, methods have been developed that exploit optimized[112] and so-called zero echo time (ZTE)[113] approaches and this has resulted in excellent MR image quality and signal in pulmonary images that is very similar to CT. Another method for measuring regional lung function involves using inhaled oxygen in combination with ^{1}H MRI[114] and this exploits the alteration of lung tissue ^{1}H relaxation times by molecular O_2. In this manner, wash-in or difference maps can be generated by using the inherent signal differences that stem from breathing room air and pure O_2. While pulmonary ventilation is reflected by O_2 wash-in maps, the alveolar-capillary transfer may be reflected by the O_2-enhancement ratio.[115] Like all ^{1}H-based MRI, O_2-enhanced MRI is limited by the weak proton signal and the fact that O_2-enhanced measurements still require histopathological validation. In fact, for all MRI measurements of COPD, validation of the pathologies directly or indirectly measured is still pending.

To tackle the challenge of very low pulmonary ^{1}H signal intensity, Bauman and colleagues[116–118] proposed another ingenious approach that relies on MRI signal oscillations that occur with the differences in lung volume during normal tidal breathing. It was hypothesized that the ^{1}H MRI signal oscillations during breathing could be employed to generate both ventilation and perfusion images. They developed a way[119] using Fourier decomposition (FD) of oscillating ^{1}H signal intensity[120] related to the compression and expansion of the lung parenchyma and blood flow[121] to generate pulmonary ventilation and/or perfusion measurements. Importantly, this method was recently shown in COPD subjects with emphysema[122] and contrast can be generated using static volumetric ^{1}H MRI methods[123]. Figure 5 shows very recent examples of FD of pulmonary magnetic resonance imaging (FDMRI) in

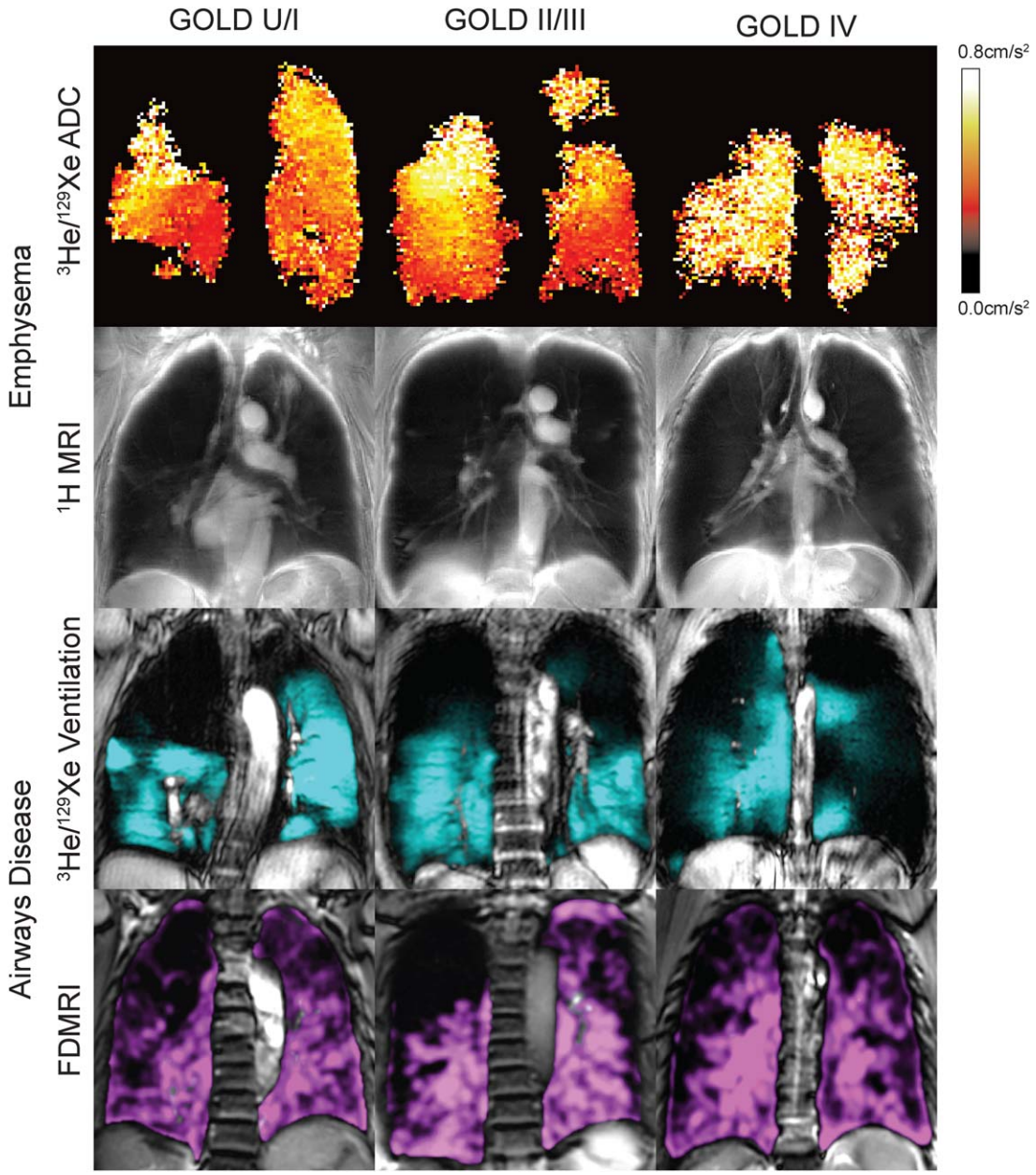

FIGURE 5: MRI measurements of COPD for different GOLD stages including: emphysema (ADC, ^{1}H MRI signal intensity), and ventilation (^{3}He MRI and FDMRI).

COPD subjects across GOLD grades and excellent comparisons were also shown in animal studies[124]. FDMRI exploits free-breathing ^{1}H MRI and nonrigid registration to generate ventilation images. Importantly, although image registration and analysis is complex, and again dependent on weak ^{1}H MRI contrast, this approach does not depend on inhaled gas or injected contrast agents, and therefore there is strong potential for clinical translation. Again, a more complete validation still needs to be undertaken.

Inhaled ^{19}F and Hyperpolarized ^{129}Xe/ ^{3}He MRI Structural and Functional Phenotypes

Similar to FD and O_2-enhanced ^{1}H MRI methods, MRI using inhaled ^{19}F gas (after multiple breaths of perfluoropropane mixed with oxygen), or hyperpolarized noble gases such as ^{3}He and ^{129}Xe (after a single breath mixed with ^{4}He or N_2), provides a way to visualize pulmonary ventilation by taking advantage of high gas density in the lung. For inhaled ^{3}He and ^{129}Xe, increased nuclear polarization generates ventilation images of the airways and airspaces and to measure apparent diffusion coefficients that estimate gas displacement. For ^{129}Xe, similar to Xe-CT methods, the fractional solubility of Xe gas in biological tissues[125] has additional applications for measuring gas exchange, alveolar surface area, and perfusion. For all three gases, the nuclear proton provides the MRI signal. In the case of ^{19}F, MR signal is inherently strong because of the high gyromagnetic ratio of ^{19}F such that extra polarization (and polarization

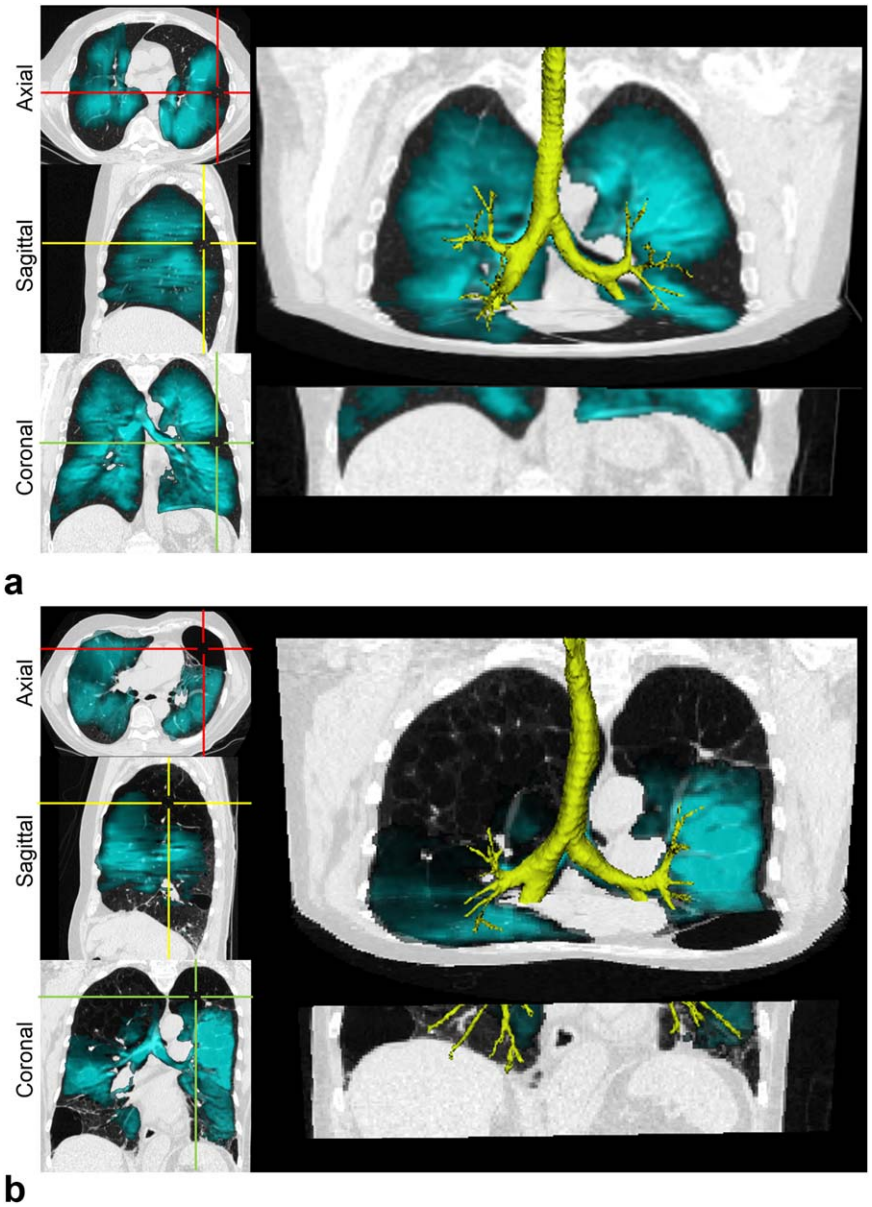

FIGURE 6: MR ventilation imaging reflecting the effects of both emphysema (slow-filling units) and airways disease (airway obstruction)—a unique predictor of COPD exacerbations in mild disease.

equipment) is not required. For both ^{3}He and ^{129}Xe, however, nuclear polarization is achieved[126,127] using laser polarization equipment. As shown in Fig. 5, ^{3}He and ^{129}Xe MRI provide superior signal-to-noise ratio ventilation images in COPD subjects, and typically, image quality using ^{3}He MRI is the greatest compared with polarized ^{129}Xe and unpolarized ^{19}F due to larger gyromagnetic ratio and high polarization rates for ^{3}He. For these reasons, currently ^{3}He MRI is most commonly used in research even though the global quantities of ^{3}He are very limited and expensive. Although experience with ^{129}Xe and ^{19}F is still limited,[128,129] these inhaled gas MRI methods provide the strongest translational potential because of the relative abundance and low cost of these gases.

Notwithstanding these challenges, recent acute therapy studies in COPD post-salbutamol[130] and post-COPD exacerbation therapy requiring hospitalization[131] show the potential for inhaled gas MRI ventilation defect measurements to represent the subtle (post-exacerbation) and not so subtle (post-salbutamol) ventilation improvements after therapy. It is important to note that the visibly obvious and statistically significant improvements in ventilation in these cases were not related to FEV_1 improvements. In addition, in a number of these previous COPD studies[132], and as shown in Fig. 6 ventilation measured using MRI was directly related to CT-derived measurements of abnormally remodeled airways and emphysema. Importantly, previous work also showed the relationship of ventilation

TABLE 1. MRI and CT COPD Phenotypes

	Imaging biomarkers of COPD		
	Airways disease	**Emphysema**	**Perfusion abnormalities**
CT	Lumen area Wall area % Pi10 PRM-gas trapping Xe gas ventilation	Low attenuating clusters Low attenuating area RA950 RA856 PRM-emphysema	Total pulmonary vascular volume Iodine perfusion
MRI	Ventilation defect percent Percent ventilated volume	ADC	Gadolinium perfusion Xe perfusion/diffusion

abnormalities with subclinical disease in smokers with normal lung function[133]. Moreover, regional ventilation worsening in COPD has been measured over a follow-up period of 2 years[134] even in patients with no change in FEV_1. The Polarized Helium Imaging of the Lung (PHIL) Study was performed in three European centers in 122 COPD patients and is the largest COPD MRI-CT multicenter comparison study completed to date[132]. This important study showed the potential for COPD biomarkers stemming from a comprehensive, prospectively planned, multicenter and multimodality imaging approach. Another innovative example[135] showed the potential of ventilation MRI to interrogate the role of regional collateral ventilation in COPD patients with bullous emphysema. Finally, MRI measurements of ventilation in mild and moderate patients (GOLD I/II COPD)[136] were also predictive of COPD exacerbation requiring hospital care, and in these patients previous exacerbation and FEV_1 were not.

For all inhaled gas MRI methods, diffusion due to random Brownian motion within the lung airways and airspaces can be measured using diffusion-weighted imaging similar to that used in conventional MRI[137]. ^{3}He or ^{129}Xe diffusion-weighted methods provide measurements of parenchyma microstructures, including the alveoli and acini that define the boundaries of the fundamental units for gas exchange[138]. The apparent diffusion coefficient (ADC) map provides quantitative regional airspace measurements information that is in agreement with the presence of emphysematous damage.[139,140] Such measurements are consistent with alveolar changes related to differences in lung volumes[141] gravitational dependence[141–143] and aging.[144] Previous COPD studies have shown that ADC correlates with pulmonary function,[142,145,146] histological measurements of lung surface area,[147] and is highly reproducible in COPD,[141] while sensitive to subclinical disease[148,149] and disease progression.[150] Novel approaches have also been used to measure diffusion in longer time frames,[151] providing a way to generate information about acinar duct and airway connectivities, including communication and collateral ventilation.[152,153] Long-range ADC appears to be more than twice as sensitive to parenchymal differences associated with COPD than short-range ADC.[154–156] Unfortunately, this important information has not yet been exploited in clinical research studies.

Gadolinium-Enhanced MRI Pulmonary Perfusion Phenotypes

Given the relative lack of ^{1}H signal in the lung using conventional approaches, gadolinium-enhanced imaging of first-pass pulmonary perfusion provides sensitive and relatively reproducible measurements of signal increase and its change over time (slope). Fourier transformation of the signal change allows for the assessment of pulmonary blood flow, mean transit time, and pulmonary blood volume. These measures can be attained over the whole lung or the lung periphery in order to evaluate microvascular perfusion.[157–159] Pulmonary perfusion deficits were observed more frequently in COPD patients as compared to healthy volunteers; the largest study to date noted largely diminished pulmonary microvascular blood flow in mild to severe COPD with strong spatial correlations in severe disease to centrilobular and panlobular emphysema[160].

Conclusion

As summarized in Table 1, pulmonary CT and MRI are on the threshold of providing regional, noninvasive measurements of ventilation, perfusion, and parenchymal destruction as intermediate endpoints of COPD. However, whereas pulmonary CT measurements have been evaluated in COPDGene,[12] ECLIPSE,[14] MESA Lung[161], CanCOLD,[15] and SPIROMICS,[13] and cardiac MRI has been utilized in over 5000 participants in MESA, pulmonary MRI has not been exploited in large-scale studies. There are many reasons for this, even though pulmonary MRI is rapid, well-tolerated, and radiation-free, so it serves as an ideal platform for serial and longitudinal evaluations in patients. More

widespread use of all imaging biomarkers has been limited for a number of key reasons, including: 1) lack of support to harmonize image acquisition software; 2) universally available image analysis software; 3) regulatory boundaries for emerging approaches; and 4) historically weak links between respiratory and radiology clinical programs. Notwithstanding these issues, as shown in Fig. 6 CT and MRI measurements of COPD are being developed to provide a better understanding of disease onset, develop COPD treatments that improve outcomes, and to provide better predictive measurements of COPD exacerbations and progression.

The unique and complementary ability of both MRI and CT to measure disease morphological and functional consequences and explore mechanisms of disease pathophysiology has not yet translated to improved COPD patient care. In COPD, there is an increasing recognition that different phenotypes exist[162–164] and that these patient groups may have different responses to therapy. Moreover, as therapies become more targeted and patient-specific, imaging will likely be one of the only ways to verify response and efficacy for an individual patient or group of patients. This will require imaging to become more quantitative, sensitive, and accessible to justify its current cost and complexity. Although the risks related to tobacco smoking will decrease over time in the developed world, as the world becomes more industrialized and polluted, and smoking habits change in the developing world, respiratory illnesses will continue to increase in prevalence, morbidity, and overall mortality. It is in this clinical context that development and appropriate utilization of pulmonary MRI and CT remain critically important.

Acknowledgments

We thank our research teams and collaborators for their continued support in the development and application of new pulmonary CT and MRI tools for the measurement and monitoring of COPD. We also thank Khadija Sheikh, Dante Capaldi, Melissa Shirk, Jered Sieren, and Ann Thompson for their assistance with figures and article preparation. This work was the result of extensive discussions during the 6th International Workshop for Pulmonary Functional Imaging, Madison, WI.

References

1. Vestbo J, Hurd SS, Agusti AG, et al. Global strategy for the diagnosis, management, and prevention of chronic obstructive pulmonary disease: GOLD executive summary. Am J Respir Crit Care Med 2013; 187:347–365.
2. Jones PW. Health status and the spiral of decline. COPD 2009;6: 59–63.
3. Milne S, King GG. Advanced imaging in COPD: insights into pulmonary pathophysiology. J Thoracic Dis 2014;6:1570–1585.
4. Sverzellati N, Molinari F, Pirronti T, Bonomo L, Spagnolo P, Zompatori M. New insights on COPD imaging via CT and MRI. Int J Chronic Obstruct Pulmon Dis 2007;2:301–312.
5. van Beek EJ, Hoffman EA. Functional imaging: CT and MRI. Clin Chest Med 2008;29:195–216,vii.
6. Hoffman EA, Simon BA, McLennan G. State of the art. A structural and functional assessment of the lung via multidetector-row computed tomography: phenotyping chronic obstructive pulmonary disease. Proc Am Thorac Soc 2006;3:519–532.
7. Galban CJ, Han MK, Boes JL, et al. Computed tomography-based biomarker provides unique signature for diagnosis of COPD phenotypes and disease progression. Nat Med 2012;18:1711–1715.
8. Castro M, Fain SB, Hoffman EA, et al. Lung imaging in asthmatic patients: the picture is clearer. J Allergy Clin Immunol 2011;128:467–478.
9. Smith BM, Hoffman EA, Rennard S, Barr RG. Location, location, location: studying anatomically comparable airways is highly relevant to understanding COPD. Thorax 2014;69:1049–1050.
10. National Lung Screening Trial Research T, Aberle DR, Berg CD, et al. The National Lung Screening Trial: overview and study design. Radiology 2011;258:243–253.
11. Barr RG, Ahmed FS, Carr JJ, et al. Subclinical atherosclerosis, airflow obstruction and emphysema: the MESA Lung Study. Eur Respir J 2012;39:846–854.
12. Regan EA, Hokanson JE, Murphy JR, et al. Genetic epidemiology of COPD (COPDGene) study design. COPD 2010;7:32–43.
13. Couper D, LaVange LM, Han MK, et al. Design of the Subpopulations and Intermediate Outcomes in COPD Study (SPIROMICS). Thorax 2013;0:1–4.
14. Faner R, Tal-Singer R, Riley JH, et al. Lessons from ECLIPSE: a review of COPD biomarkers. Thorax 2014;69:666–672.
15. Bourbeau J, Tan WC, Benedetti A, et al. Canadian Cohort Obstructive Lung Disease (CanCOLD): fulfilling the need for longitudinal observational studies in COPD. COPD 2014;11:125–132.
16. Adams H, Bernard M, McConnochie K. An appraisal of CT pulmonary density mapping in normal subjects. Clin Radiol 1991;43:238–242.
17. Kinsella M, Muller NL, Abboud RT, Morrison NJ, DyBuncio A. Quantitation of emphysema by computed tomography using a "density mask" program and correlation with pulmonary function tests. Chest 1990;97:315–321.
18. Muller NL, Staples CA, Miller RR, Abboud RT. "Density mask." An objective method to quantitate emphysema using computed tomography. Chest 1988;94:782–787.
19. Gould GA, Macnee W, McLean A, et al. CT Measurements of Lung Density in Life can quantitate distal airspace enlargement–an essential defining feature of human emphysema. Am Rev Resp Dis 1988;137: 380–392.
20. Hartley PG, Galvin JR, Hunninghake GW, et al. High-resolution CT-derived measures of lung density are valid indexes of interstitial lung disease. J Appl Physiol 1994;76:271–277.
21. Coxson HO, Rogers RM. Quantitative computed tomography of chronic obstructive pulmonary disease. Acad Radiol 2005;12:1457–1463.
22. Newell JD Jr, Hogg JC, Snider GL. Report of a workshop: quantitative computed tomography scanning in longitudinal studies of emphysema. Eur Respir J 2004;23:769–775.
23. Stolk J, Ng WH, Bakker ME, et al. Correlation between annual change in health status and computer tomography derived lung density in subjects with alpha1-antitrypsin deficiency. Thorax 2003;58:1027–1030.
24. Coxson HO. Quantitative chest tomography in COPD research: chairman's summary. Proc Am Thorac Soc 2008;5:874–877.
25. Hoffman EA, Simon BA, McLennan G. State of the art. A structural and functional assessment of the lung via multidetector-row

computed tomography: phenotyping chronic obstructive pulmonary disease. Proc Am Thorac Soc 2006;3:519–532.

26. Fishman A, Martinez F, Naunheim K, et al. A randomized trial comparing lung-volume-reduction surgery with medical therapy for severe emphysema. N Engl J Med 2003;348:2059–2073.
27. Tschirren J, Hoffman EA, McLennan G, Sonka M. Intrathoracic airway trees: segmentation and airway morphology analysis from low-dose CT scans. IEEE Trans Med Imaging 2005;24:1529–1539.
28. Tschirren J, McLennan G, Palagyi K, Hoffman EA, Sonka M. Matching and anatomical labeling of human airway tree. IEEE Trans Med Imaging 2005;24:1540–1547.
29. Cho MH, Washko GR, Hoffmann TJ, et al. Cluster analysis in severe emphysema subjects using phenotype and genotype data: an exploratory investigation. Respir Res 2010;11:30.
30. Manichaikul A, Hoffman EA, Smolonska J, et al. Genome-wide study of percent emphysema on computed tomography in the general population. The Multi-Ethnic Study of Atherosclerosis Lung/SNP Health Association Resource Study. Am J Respir Crit Care Med 2014;189:408–418.
31. Barr RG, Bluemke DA, Ahmed FS, et al. Percent emphysema, airflow obstruction, and impaired left ventricular filling. N Engl J Med 2010; 362:217–227.
32. Washko GR, Martinez FJ, Hoffman EA, et al. Physiological and computed tomographic predictors of outcome from lung volume reduction surgery. Am J Respir Crit Care Med 2010;181:494–500.
33. Washko GR, Criner GJ, Mohsenifar Z, et al. Computed tomographic-based quantification of emphysema and correlation to pulmonary function and mechanics. COPD 2008;5:177–186.
34. Lovasi GS, Diez Roux AV, Hoffman EA, Kawut SM, Jacobs DR Jr, Barr RG. Association of environmental tobacco smoke exposure in childhood with early emphysema in adulthood among nonsmokers: the MESA-lung study. Am J Epidemiol 2010;171:54–62.
35. Han MK, Wise R, Mumford J, et al. Prevalence and clinical correlates of bronchoreversibility in severe emphysema. Eur Respir J 2010;35: 1048–1056.
36. Lederer DJ, Enright PL, Kawut SM, et al. Cigarette smoking is associated with subclinical parenchymal lung disease: the Multi-Ethnic Study of Atherosclerosis (MESA)-lung study. Am J Respir Crit Care Med 2009;180:407–414.
37. Busacker A, Newell JD Jr, Keefe T, et al. A multivariate analysis of risk factors for the air-trapping asthmatic phenotype as measured by quantitative CT analysis. Chest 2009;135:48–56.
38. Mishima M, Hirai T, Itoh H, et al. Complexity of terminal airspace geometry assessed by lung computed tomography in normal subjects and patients with chronic obstructive pulmonary disease. Proc Natl Acad Sci U S A 1999;96:8829–8834.
39. Xu Y, Sonka M, McLennan G, Guo J, Hoffman EA. MDCT-based 3-D texture classification of emphysema and early smoking related lung pathologies. IEEE Trans Med Imaging 2006;25:464–475.
40. Madani A, Van Muylem A, de Maertelaer V, Zanen J, Gevenois PA. Pulmonary emphysema: size distribution of emphysematous spaces on multidetector CT images—comparison with macroscopic and microscopic morphometry. Radiology 2008;248:1036–1041.
41. Gietema HA, Muller NL, Fauerbach PV, et al. Quantifying the extent of emphysema: factors associated with radiologists' estimations and quantitative indices of emphysema severity using the ECLIPSE cohort. Acad Radiol 2011;18:661–671.
42. Stoel BC, Bakker ME, Stolk J, et al. Comparison of the sensitivities of 5 different computed tomography scanners for the assessment of the progression of pulmonary emphysema: a phantom study. Invest Radiol 2004;39:1–7.
43. Shaker SB, Dirksen A, Laursen LC, Skovgaard LT, Holstein-Rathlou NH. Volume adjustment of lung density by computed tomography scans in patients with emphysema. Acta Radiol 2004;45:417–423.
44. Boedeker KL, McNitt-Gray MF, Rogers SR, et al. Emphysema: effect of reconstruction algorithm on CT imaging measures. Radiology 2004;232:295–301.
45. Sieren JP, Newell JD, Judy PF, et al. Reference standard and statistical model for intersite and temporal comparisons of CT attenuation in a multicenter quantitative lung study. Med Phys 2012;39:5757–5767.
46. Hoffman EA, Barr R. Thresholds to Lung Density Measures Hoffman and Barr Replies. Acad Radiol 2010;17:339–401.
47. Hoffman EA, Ahmed FS, Baumhauer H, et al. Variation in the percent of emphysema-like lung in a healthy, nonsmoking multiethnic sample. The MESA lung study. Ann Am Thorac Soc 2014;11:898–907.
48. Newell JD Jr, Fuld MK, Allmendinger T, et al. Very low-dose (0.15 mGy) chest CT protocols using the COPDGene 2 test object and a third-generation dual-source CT scanner with corresponding third-generation iterative reconstruction software. Invest Radiol 2015;50: 40–45.
49. Sieren JP, Hoffman EA, Fuld MK, Chan KS, Guo J, Newell JD Jr. Sinogram Affirmed Iterative Reconstruction (SAFIRE) versus weighted filtered back projection (WFBP) effects on quantitative measure in the COPDGene 2 test object. Med Phys 2014;41:091910.
50. Pontana F, Pagniez J, Flohr T, et al. Chest computed tomography using iterative reconstruction vs filtered back projection. Part 1. Evaluation of image noise reduction in 32 patients. Eur Radiol 2011;21: 627–635.
51. Yanagawa M, Honda O, Yoshida S, et al. Adaptive statistical iterative reconstruction technique for pulmonary CT: image quality of the cadaveric lung on standard- and reduced-dose CT. Acad Radiol 2010; 17:1259–1266.
52. Honda O, Yanagawa M, Inoue A, et al. Image quality of multiplanar reconstruction of pulmonary CT scans using adaptive statistical iterative reconstruction. Br J Radiol 2011;84:335–341.
53. Heilbron BG, Leipsic J. Submillisievert coronary computed tomography angiography using adaptive statistical iterative reconstruction — a new reality. Can J Cardiol 2010;26:35–36.
54. Moscariello A, Takx RA, Schoepf UJ, et al. Coronary CT angiography: image quality, diagnostic accuracy, and potential for radiation dose reduction using a novel iterative image reconstruction technique-comparison with traditional filtered back projection. Eur Radiol 2011; 21:2130–2138.
55. McCollough CH, Chen GH, Kalender W, et al. Achieving routine submillisievert CT scanning: report from the summit on management of radiation dose in CT. Radiology 2012;264:567–580.
56. Coxson HO, Leipsic J, Parraga G, Sin DD. Using pulmonary imaging to move chronic obstructive pulmonary disease beyond FEV1. Am J Respir Crit Care Med 2014;190:135–144.
57. Hoffman EA, Clough AV, Christensen GE, et al. The comprehensive imaging-based analysis of the lung: a forum for team science. Acad Radiol 2004;11:1370–1380.
58. Jarjour NN, Erzurum SC, Bleecker ER, et al. Severe asthma: lessons learned from the National Heart, Lung, and Blood Institute Severe Asthma Research Program. Am J Respir Crit Care Med 2012;185:356–362.
59. Coxson HO, Dirksen A, Edwards LD, et al. The presence and progression of emphysema in COPD as determined by CT scanning and biomarker expression: a prospective analysis from the ECLIPSE study. Lancet Respir Med 2013;1:129–136.
60. Coxson HO. Using computed tomography to measure the site of airflow obstruction. Respirology 2012;17:5–6.
61. Coxson HO. Quantitative chest tomography in COPD research: chairman's summary. Proc Am Thorac Soc 2008;5:874–877.
62. Pauwels RA, Buist AS, Calverley PM, Jenkins CR, Hurd SS, Committee GS. Global strategy for the diagnosis, management, and prevention of chronic obstructive pulmonary disease. NHLBI/WHO Global Initiative for Chronic Obstructive Lung Disease (GOLD) Workshop summary. Am J Respir Crit Care Med 2001;163:1256–1276.
63. Wright JL, Churg A. Advances in the pathology of COPD. Histopathology 2006;49:1–9.
64. Peinado VI, Ramirez J, Roca J, Rodriguez-Roisin R, Barbera JA. Identification of vascular progenitor cells in pulmonary arteries of patients

with chronic obstructive pulmonary disease. Am J Respir Cell Mol Biol 2006;34:257–263.

65. Ishizawa K, Kubo H, Yamada M, et al. Bone marrow-derived cells contribute to lung regeneration after elastase-induced pulmonary emphysema. FEBS Lett 2004;556:249–252.

66. Remy-Jardin M, Edme JL, Boulenguez C, Remy J, Mastora I, Sobaszek A. Longitudinal follow-up study of smoker's lung with thin-section CT in correlation with pulmonary function tests. Radiology 2002;222:261–270.

67. Gust R, Kozlowski J, Stephenson AH, Schuster DP. Synergistic hemodynamic effects of low-dose endotoxin and acute lung injury. Am J Respir Crit Care Med 1998;157(6 Pt 1):1919–1926.

68. Schuster DP, Marklin GF. The effect of regional lung injury or alveolar hypoxia on pulmonary blood flow and lung water measured by positron emission tomography. Am Rev Respir Dis 1986;133:1037–1042.

69. Easley RB, Fuld MK, Fernandez-Bustamante A, Hoffman EA, Simon BA. Mechanism of hypoxemia in acute lung injury evaluated by multidetector-row CT. Acad Radiol 2006;13:916–921.

70. Alford SK, van Beek EJ, McLennan G, Hoffman EA. Heterogeneity of pulmonary perfusion as a mechanistic image-based phenotype in emphysema susceptible smokers. Proc Natl Acad Sci U S A 2010;107:7485–7490.

71. Vonk-Noordegraaf A. The shrinking heart in chronic obstructive pulmonary disease. N Engl J Med 2010;362:267–268.

72. Fuld MK, Halaweish AF, Haynes SE, Divekar AA, Guo J, Hoffman EA. Pulmonary perfused blood volume with dual-energy CT as surrogate for pulmonary perfusion assessed with dynamic multidetector CT. Radiology 2013;267:747–756.

73. Chon D, Beck KC, Simon BA, Shikata H, Saba OI, Hoffman EA. Effect of low-xenon and krypton supplementation on signal/noise of regional CT-based ventilation measurements. J Appl Physiol 2007;102:1535–1544.

74. Chon D, Simon BA, Beck KC, et al. Differences in regional wash-in and wash-out time constants for xenon-CT ventilation studies. Respir Physiol Neurobiol 2005;148:65–83.

75. Hoffman EA, Chon D. Computed tomography studies of lung ventilation and perfusion. Proc Am Thorac Soc 2005;2:\492–498, 506.

76. MK F, Simon BA, Van Beek EJ, Hudson M, Sieren J, Hoffman EA. Transitioning from the laboratory to the clinic: adapting the Xe-CT method for human scanning. American Thoracic Society Annual Meeting; 2008; Toronto, Canada.

77. Fuld M, van Beek E, Simon B, Morgan J, Hoffman EA. Establishing "normal" regional ventilation via dynamic xenon-CT in humans. American Thoracic Annual Meeting; 2009; San Diego, CA.

78. Park HW, Jung JW, Kim KM, et al. Xenon ventilation computed tomography and the management of asthma in the elderly. Respirology 2014;19:389–395.

79. Kong X, Sheng HX, Lu GM, et al. Xenon-enhanced dual-energy CT lung ventilation imaging: techniques and clinical applications. AJR Am J Roentgenol 2014;202:309–317.

80. Park EA, Goo JM, Park SJ, et al. Chronic obstructive pulmonary disease: quantitative and visual ventilation pattern analysis at xenon ventilation CT performed by using a dual-energy technique. Radiology 2010;256:985–997.

81. Chae EJ, Seo JB, Goo HW, et al. Xenon ventilation CT with a dual-energy technique of dual-source CT: initial experience. Radiology 2008;248:615–624.

82. Jung JW, Kwon JW, Kim TW, et al. New insight into the assessment of asthma using xenon ventilation computed tomography. Ann Allergy Asthma Immunol 2013;111:90–95 e92.

83. Fuld MK, Halaweish AF, Newell JD Jr, Krauss B, Hoffman EA. Optimization of dual-energy xenon-computed tomography for quantitative assessment of regional pulmonary ventilation. Invest Radiol 2013;48:629–637.

84. Mahnken AH, Jost G, Pietsch H. Krypton for computed tomography lung ventilation imaging: preliminary animal data. Invest Radiol 2015;50:305–308.

85. Hachulla AL, Pontana F, Wemeau-Stervinou L, et al. Krypton ventilation imaging using dual-energy CT in chronic obstructive pulmonary disease patients: initial experience. Radiology 2012;263:253–259.

86. Schmidt TG, Zimmerman KC, Sidky EY. The effects of extending the spectral information acquired by a photon-counting detector for spectral CT. Phys Med Biol 2015;60:1583–1600.

87. de Vries A, Roessl E, Kneepkens E, et al. Quantitative spectral K-edge imaging in preclinical photon-counting x-ray computed tomography. Invest Radiol 2014;ss:22–22.

88. Lee S, Choi YN, Kim HJ. Quantitative material decomposition using spectral computed tomography with an energy-resolved photon-counting detector. Phys Med Biol 2014;59:5457–5482.

89. Fuld MK, Easley RB, Saba OI, et al. CT-measured regional specific volume change reflects regional ventilation in supine sheep. J Appl Physiol (1985) 2008;104:1177–1184.

90. Ding K, Cao K, Fuld MK, et al. Comparison of image registration based measures of regional lung ventilation from dynamic spiral CT with Xe-CT. Med Phys 2012;39:5084–5098.

91. Yin Y, Hoffman EA, Ding K, Reinhardt JM, Lin CL. A cubic B-spline-based hybrid registration of lung CT images for a dynamic airway geometric model with large deformation. Phys Med Biol 2011;56:203–218.

92. Yin Y, Choi J, Hoffman EA, Tawhai MH, Lin CL. A multiscale MDCT image-based breathing lung model with time-varying regional ventilation. J Computat Phys 2013;244:168–192.

93. Choi S, Hoffman EA, Wenzel S, et al. Registration-based assessment of regional lung function via volumetric CT images of normal vs. severe asthmatics. J Appl Physiol 2013;115:730–742.

94. Yin Y, Hoffman EA, Lin CL. Lung lobar slippage assessed with the aid of image registration. Med Image Comput Comput Assist Intervent 2010;13(Pt 2):578–585.

95. Jahani N, Yin Y, Hoffman EA, Lin CL. Assessment of regional nonlinear tissue deformation and air volume change of human lungs via image registration. J Biomech 2014;47:1626–1633.

96. Schroeder JD, McKenzie AS, Zach JA, et al. Relationships between airflow obstruction and quantitative CT measurements of emphysema, air trapping, and airways in subjects with and without chronic obstructive pulmonary disease. AJR Am J Roentgenol 2013;201:W460–470.

97. Mets OM, Buckens CF, Zanen P, et al. Identification of chronic obstructive pulmonary disease in lung cancer screening computed tomographic scans. JAMA 2011;306:1775–1781.

98. McDonough JE, Yuan R, Suzuki M, et al. Small-airway obstruction and emphysema in chronic obstructive pulmonary disease. N Engl J Med 2011;365:1567–1575.

99. Estepar RS, Kinney GL, Black-Shinn JL, et al. Computed tomographic measures of pulmonary vascular morphology in smokers and their clinical implications. Am J Respir Crit Care Med 2013;188:231–239.

100. Gao Z, Grout RW, Holtze C, Hoffman EA, Saha PK. A new paradigm of interactive artery/vein separation in noncontrast pulmonary CT imaging using multiscale topomorphologic opening. IEEE Trans Biomed Eng 2012;59:3016–3027.

101. Saha PK, Gao Z, Alford SK, Sonka M, Hoffman EA. Topomorphologic separation of fused isointensity objects via multiscale opening: separating arteries and veins in 3-D pulmonary CT. IEEE Trans Med Imaging 2010;29:840–851.

102. Wells JM, Washko GR, Han MK, et al. Pulmonary arterial enlargement and acute exacerbations of COPD. N Engl J Med 2012;367:913–921.

103. Barr RG. The epidemiology of vascular dysfunction relating to chronic obstructive pulmonary disease and emphysema. Proc Am Thorac Soc 2011;8:522–527.

104. Ley-Zaporozhan J, Ley S, Kauczor HU. Proton MRI in COPD. COPD 2007;4:55–65.

105. Vogel-Claussen J, Renne J, Hinrichs J, et al. Quantification of pulmonary inflammation after segmental allergen challenge using TIRM magnetic resonance imaging. Am J Respir Crit Care Med 2014;189:650–657.

106. Mayo JR, MacKay A, Muller NL. MR imaging of the lungs: value of short TE spin-echo pulse sequences. AJR Am J Roentgenol 1992; 159:951–956.

107. Mayo JR. Thoracic magnetic resonance imaging: physics and pulse sequences. J Thorac Imaging 1993;8:1–11.

108. Ma W, Sheikh K, Svenningsen S, et al. Ultra-short echo-time pulmonary MRI: evaluation and reproducibility in COPD subjects with and without bronchiectasis. J Magn Reson Imaging 2015;41:1465–1474.

109. Takahashi M, Togao O, Obara M, et al. Ultra-short echo time (UTE) MR imaging of the lung: comparison between normal and emphysematous lungs in mutant mice. J Magn Reson Imaging JMRI 2010; 32:326–333.

110. Zurek M, Boyer L, Caramelle P, Boczkowski J, Crémillieux Y. Longitudinal and noninvasive assessment of emphysema evolution in a murine model using proton MRI. Magn Reson Med 2012;68:898–904.

111. Ohno Y, Koyama H, Yoshikawa T, et al. T2* measurements of 3-T MRI with ultrashort TEs: capabilities of pulmonary function assessment and clinical stage classification in smokers. AJR Am J Roentgenol 2011;197:W279–285.

112. Johnson KM, Fain SB, Schiebler ML, Nagle S. Optimized 3D ultrashort echo time pulmonary MRI. Magn Reson Med 2013;70:1241–1250.

113. Weiger M, Wu M, Wurnig MC, et al. Rapid and robust pulmonary proton ZTE imaging in the mouse. NMR Biomed 2014;27:1129–1134.

114. Edelman RR, Hatabu H, Tadamura E, Li W, Prasad PV. Noninvasive assessment of regional ventilation in the human lung using oxygen-enhanced magnetic resonance imaging. Nat Med 1996;2:1236–1239.

115. Ohno Y, Koyama H, Nogami M, et al. Dynamic oxygen-enhanced MRI versus quantitative CT: pulmonary functional loss assessment and clinical stage classification of smoking-related COPD. AJR Am J Roentgenol 2008;190:W93–99.

116. Bauman G, Puderbach M, Deimling M, et al. Non-contrast-enhanced perfusion and ventilation assessment of the human lung by means of fourier decomposition in proton MRI. Magn Reson.Med 2009;62: 656–664.

117. Bauman G, Lutzen U, Ullrich M, et al. Pulmonary functional imaging: qualitative comparison of Fourier decomposition MR imaging with SPECT/CT in porcine lung. Radiology 2011;260:551–559.

118. Biederer J, Mirsadraee S, Beer M, et al. MRI of the lung (3/3)-current applications and future perspectives. Insights Imaging 2012;3:373–386.

119. Chefd'hotel C HG, Faugeras O. A variational approach to multimodal image matching. In: Proceedings of the IEEE Workshop on Variational and Level Set Methods in Computer Vision (VLSM'2001); 2001; Vancouver, British Columbia, Canada.

120. Deimling M JV, Geiger B, Chefd'Hotel C. Time resolved lung ventilation imaging by Fourier decomposition. In: Proc 16th Annual Meeting ISMRM, Toronto; 2008.

121. Bauman G, Puderbach M, Deimling M, et al. Non-contrast-enhanced perfusion and ventilation assessment of the human lung by means of fourier decomposition in proton MRI. Magn Reson Med 2009;62: 656–664.

122. Capaldi DP, Sheikh K, Guo F, et al. Free-breathing pulmonary 1H and hyperpolarized He MRI: comparison in COPD and bronchiectasis. Acad Radiol 2014;22:320–329.

123. Pennati F, Quirk JD, Yablonskiy DA, Castro M, Aliverti A, Woods JC. Assessment of regional lung function with multivolume (1)H MR imaging in health and obstructive lung disease: comparison with (3)He MR imaging. Radiology 2014;273:580–590.

124. Bauman G, Scholz A, Rivoire J, et al. Lung ventilation- and perfusion-weighted Fourier decomposition magnetic resonance imaging: in vivo validation with hyperpolarized 3He and dynamic contrast-enhanced MRI. Magn Reson Med 2013;69:229–237.

125. MacDonald A, Wann K. Physiological aspects of anaesthetics and inert gases. London: Academic Press; 1978.

126. Goodson BM. Nuclear magnetic resonance of laser-polarized noble gases in molecules, materials, and organisms. J Magn Reson 2002; 155:157–216.

127. Saam BT. Magnetic resonance imaging with laser-polarized noble gases. Nat Med 1996;2:358–359.

128. Halaweish AF, Moon RE, Foster WM, et al. Perfluoropropane gas as a magnetic resonance lung imaging contrast agent in humans. Chest 2013;144:1300–1310.

129. Couch MJ, Ball IK, Li T, et al. Pulmonary ultrashort echo time 19F MR imaging with inhaled fluorinated gas mixtures in healthy volunteers: feasibility. Radiology 2013;269:903–909.

130. Kirby M, Mathew L, Heydarian M, Etemad-Rezai R, McCormack DG, Parraga G. Chronic obstructive pulmonary disease: quantification of bronchodilator effects by using hyperpolarized He MR imaging. Radiology 2011;281:283–292.

131. Kirby M, Kanhere N, Etemad-Rezai R, McCormack DG, Parraga G. Hyperpolarized helium-3 magnetic resonance imaging of chronic obstructive pulmonary disease exacerbation. J Magn Reson Imaging 2013;37:1223–1227.

132. Van Beek EJ, Dahmen AM, Stavngaard T, et al. Hyperpolarised 3He MRI versus HRCT in COPD and normal volunteers: PHIL trial. Eur Respir J 2009;34:1311–1321.

133. Woodhouse N, Wild JM, Paley MN, et al. Combined helium-3/proton magnetic resonance imaging measurement of ventilated lung volumes in smokers compared to never-smokers. J Magn Reson Imaging 2005;21:365–369.

134. Kirby M, Mathew L, Wheatley A, Santyr GE, McCormack DG, Parraga G. Chronic obstructive pulmonary disease: longitudinal hyperpolarized (3)He MR imaging. Radiology 2010;256:280–289.

135. Marshall H, Deppe MH, Parra-Robles J, et al. Direct visualisation of collateral ventilation in COPD with hyperpolarised gas MRI. Thorax 2012;67:612–617.

136. Kirby M, Pike D, Coxson HO, McCormack DG, Parraga G. Hyperpolarized (3)He ventilation defects used to predict pulmonary exacerbations in mild to moderate chronic obstructive pulmonary disease. Radiology 2014;273:887–896.

137. Basser PJ, Mattiello J, LeBihan D. Estimation of the effective self-diffusion tensor from the NMR spin echo. J Magn Reson B 1994;103: 247–254.

138. Saam B, Yablonskiy D, Kodibagkar V, et al. MR imaging of diffusion of ^{3}He gas in healthy and diseased lungs. Magn Reson Med 2000; 44:174–179.

139. Brookeman J, Mugler JP 3rd, Knight-Scott J, Munger T, deLange E, Bogorad P. Studies of 3He diffusion coefficient in the human lung: age-related distribution patterns. Eur J Radiol 1999;9:21.

140. Kauczor HU, Ebert M, Kreitner KF, et al. Imaging of the lungs using 3He MRI: preliminary clinical experience in 18 patients with and without lung disease. J Magn Reson Imaging 1997;7:538–543.

141. Diaz S, Casselbrant I, Piitulainen E, et al. Hyperpolarized ^{3}He apparent diffusion coefficient MRI of the lung: reproducibility and volume dependency in healthy volunteers and patients with emphysema. J Magn Reson Imaging 2008;27:763–770.

142. Morbach AE, Gast KK, Schmiedeskamp J, et al. Diffusion-weighted MRI of the lung with hyperpolarized helium-3: a study of reproducibility. J Magn Reson Imaging 2005;21:765–774.

143. Fichele S, Woodhouse N, Swift AJ, et al. MRI of helium-3 gas in healthy lungs: posture related variations of alveolar size. J Magn Reson Imaging 2004;20:331–335.

144. Fain SB, Altes TA, Panth SR, et al. Detection of age-dependent changes in healthy adult lungs with diffusion-weighted ^{3}He MRI. Acad Radiol 2005;12:1385–1393.

145. Salerno M, de Lange EE, Altes TA, Truwit JD, Brookeman JR, Mugler JP 3rd. Emphysema: hyperpolarized helium 3 diffusion MR

imaging of the lungs compared with spirometric indexes—initial experience. Radiology 2002;222:252–260.

146. Diaz S, Casselbrant I, Piitulainen E, et al. Validity of apparent diffusion coefficient hyperpolarized ^{3}He-MRI using MSCT and pulmonary function tests as references. Eur J Radiol 2009;71:257–263.

147. Woods JC, Choong CK, Yablonskiy DA, et al. Hyperpolarized 3He diffusion MRI and histology in pulmonary emphysema. Magn Reson Med 2006;56:1293–1300.

148. Fain SB, Panth SR, Evans MD, et al. Early emphysematous changes in asymptomatic smokers: detection with ^{3}He MR imaging. Radiology 2006;239:875–883.

149. Swift AJ, Wild JM, Fichele S, et al. Emphysematous changes and normal variation in smokers and COPD patients using diffusion 3He MRI. Eur.J.Radiol 2005;54:352–358.

150. Diaz S, Casselbrant I, Piitulainen E, et al. Progression of emphysema in a 12-month hyperpolarized 3He-MRI study: lacunarity analysis provided a more sensitive measure than standard ADC analysis. Acad Radiol 2009;16:700–707.

151. Wang C, Miller GW, Altes TA, de Lange EE, Cates GD Jr, Mugler JP 3rd. Time dependence of 3He diffusion in the human lung: measurement in the long-time regime using stimulated echoes. Magn Reson Med 2006;56:296–309.

152. Bartel SE, Haywood SE, Woods JC, et al. Role of collateral paths in long-range diffusion in lungs. J Appl Physiol 2008;104:1495–1503.

153. Conradi MS, Yablonskiy DA, Woods JC, et al. The role of collateral paths in long-range diffusion of 3He in lungs. Acad Radiol 2008;15:675–682.

154. Woods JC, Yablonskiy DA, Choong CK, et al. Long-range diffusion of hyperpolarized 3He in explanted normal and emphysematous human lungs via magnetization tagging. J Appl Physiol 2005;99:1992–1997.

155. Wang C, Altes TA, Mugler JP 3rd, et al. Assessment of the lung microstructure in patients with asthma using hyperpolarized 3He diffusion MRI at two time scales: comparison with healthy subjects and patients with COPD. J Magn Reson Imaging 2008;28:80–88.

156. Wang C, Miller GW, Altes TA, et al. Extending the range of diffusion times for regional measurement of the 3He ADC in human lungs. Magn Reson Med 2008;59:673–678.

157. Fan L, Xia Y, Guan Y, et al. Capability of differentiating smokers with normal pulmonary function from COPD patients: a comparison of CT pulmonary volume analysis and MR perfusion imaging. Eur Radiol 2013;23:1234–1241.

158. Fan L, Xia Y, Guan Y, Zhang TF, Liu SY. Characteristic features of pulmonary function test, CT volume analysis and MR perfusion imaging in COPD patients with different HRCT phenotypes. Clin Respir J 2014;8:45–54.

159. Xia Y, Guan Y, Fan L, et al. Dynamic contrast enhanced magnetic resonance perfusion imaging in high-risk smokers and smoking-related COPD: correlations with pulmonary function tests and quantitative computed tomography. COPD 2014;11:510–520.

160. Sergiacomi G, Taglieri A, Chiaravalloti A, et al. Acute COPD exacerbation: 3 T MRI evaluation of pulmonary regional perfusion—preliminary experience. Respir Med 2014;108:875–882.

161. Barr RG, Bluemke DA, Ahmed FS, et al. Percent emphysema, airflow obstruction, and impaired left ventricular filling. N Engl J Med 2010;362:217–227.

162. Moore WC, Bleecker ER, Curran-Everett D, et al. Characterization of the severe asthma phenotype by the National Heart, Lung, and Blood Institute's Severe Asthma Research Program. J Allergy Clin Immunol 2007;119:405–413.

163. Mathew L, Kirby M, Etemad-Rezai R, Wheatley A, McCormack DG, Parraga G. Hyperpolarized (3)He magnetic resonance imaging: preliminary evaluation of phenotyping potential in chronic obstructive pulmonary disease. Eur J Radiol 2011;79:140–146.

164. Coxson HO, Mayo J, Lam S, Santyr G, Parraga G, Sin DD. New and current clinical imaging techniques to study chronic obstructive pulmonary disease. Am J Respir Crit Care Med 2009;180:588–597.